A Study of Ice-rafted Debris as a Paleoclimatic Proxy for the North Atlantic for the Last One Million Years.

A Senior Thesis

Submitted as Partial Fulfillment of the Requirements

for the degree Bachelor of Science in

Geological Sciences at

The Ohio State University

by

Margaret E. Haack

The Ohio State University, Spring Quarter 2006

Approved by:

Lawrence Krissek

Dr. Lawrence A. Krissek

Table of Contents

Abstract

Discovering the reasons for abrupt climate changes is one of the major challenges in global climate research today. Through the use of $\delta^{18}O$ isotope records from ice cores in Greenland and marine sediment records from cores drilled in the North Atlantic, more detailed records of paleoclimate proxies for the North Atlantic can be established. Samples taken from sediment cores drilled off the southeastern coast of Greenland at Site 1305 from IODP Expedition 303 were used to develop a millennial-scale record of sediments transported into the North Atlantic by icebergs.

The objective of this study was to determine the IRD input history at Site 1305 for the last one million years. Approximately 200 samples were analyzed for the abundance of ice-rafted debris (IRD) present in each sample. For this study, IRD is defined as the lithic grains in the > 150 μm sand fraction. The abundance of IRD was determined as the weight percent of the > 150 μm sand fraction relative to the total bulk weight.

The IRD weight percent was plotted versus the age of the sample. The sample ages were determined using an age-depth model constructed by the 303 Scientific Party. For Site 1305, distributed throughout the record there are a series of large IRD maxima that range from 1.16 to 13.37 weight percent (wt %). The major IRD peaks did not occur in the middle of glacial or interglacial stages, nor did most of them straddle a glacial/interglacial transition. Instead, the IRD maxima were positioned just before (average lead of 32.3 k.y.) or just after (average lag of 6.7 k.y.) the onset of glaciation.

Site 1305 provides evidence to suggest that ice-rafting occurred during the early stages of global ice increase; local controls, not just global ones, were affecting ice production and transport of icebergs. The data from Site 1305 indicate the following:

- no evidence of any long term trends in IRD abundance
- an apparent 100,000 year cyclicity in the largest peaks
- IRD maxima do not correlate directly to stage boundaries over the last one million years. The last observation may be the result of differences in the sources of the signals (local for IRD; global ice volume for the isotope stages), a transition from easily eroded surface materials to more competent bedrock during a glacial advance, and changes in the volume and presence of sea ice.

Further work for this study will be to analyze the remainder of the existing samples, fill in gaps in the data set in order to possibly observe sub- Milankovitch events, and examine the grain composition of the IRD to identify iceberg sources.

Acknowledgements

I would like to thank my advisor, Dr. Lawrence Krissek, for all his contributions and guidance throughout the entire research process. This research used samples and/or data provided by the Integrated Ocean Drilling Program (IODP) Expedition 303. The IODP is sponsored by the U.S. National Science Foundation (NSF) and participating countries under management of Joint Oceanographic Institutions (JOI), Inc. Funding for this research was provided by the U.S. Science Support Program.

1. Introduction

The North Atlantic is a climatically sensitive region on Earth, due to the interactions between the ocean, atmosphere, and cryosphere (i.e., glaciers) that have occurred there on timescales of tens of thousands to hundred of thousands of years. In addition, the North Atlantic appears to be prone to periods of abrupt climate change (on the order of thousands of years or less). Understanding the mechanisms and causes of such episodes of abrupt climate change is one of the major challenges in global climate change research today. However, records with sufficient detail to reveal episodes of abrupt climate change only extend back for several tens of thousands of years. As a result, research in abrupt climate change requires the development of longer and more detailed records of paleoclimatic proxies (i.e., sediment components that carry information about past oceanographic, atmospheric, and glacial conditions). Previous studies have been instrumental in developing marine records of millennial-scale climate variations, and this study is a step toward developing a millennial-scale record of sediments transported from land into the North Atlantic by icebergs (i.e., ice-rafted debris or IRD). Increases in the abundance of IRD are interpreted to record times of glacial expansion to sea level (when icebergs can be released), and the composition of the IRD can be used to identify the source area(s) and/or the dispersal trajectory of those icebergs.

2. Background

Evidence from $\delta^{18}O$ isotope records for Ice evolution

Episodic pulses of IRD were among the first clues of subpolar variations in glacial cycles in the North Atlantic (McManus et al, 1999), and much has been learned about natural climate variations through the study of ice and sediment cores (Figure 1; Raymo et al., 1998). In the

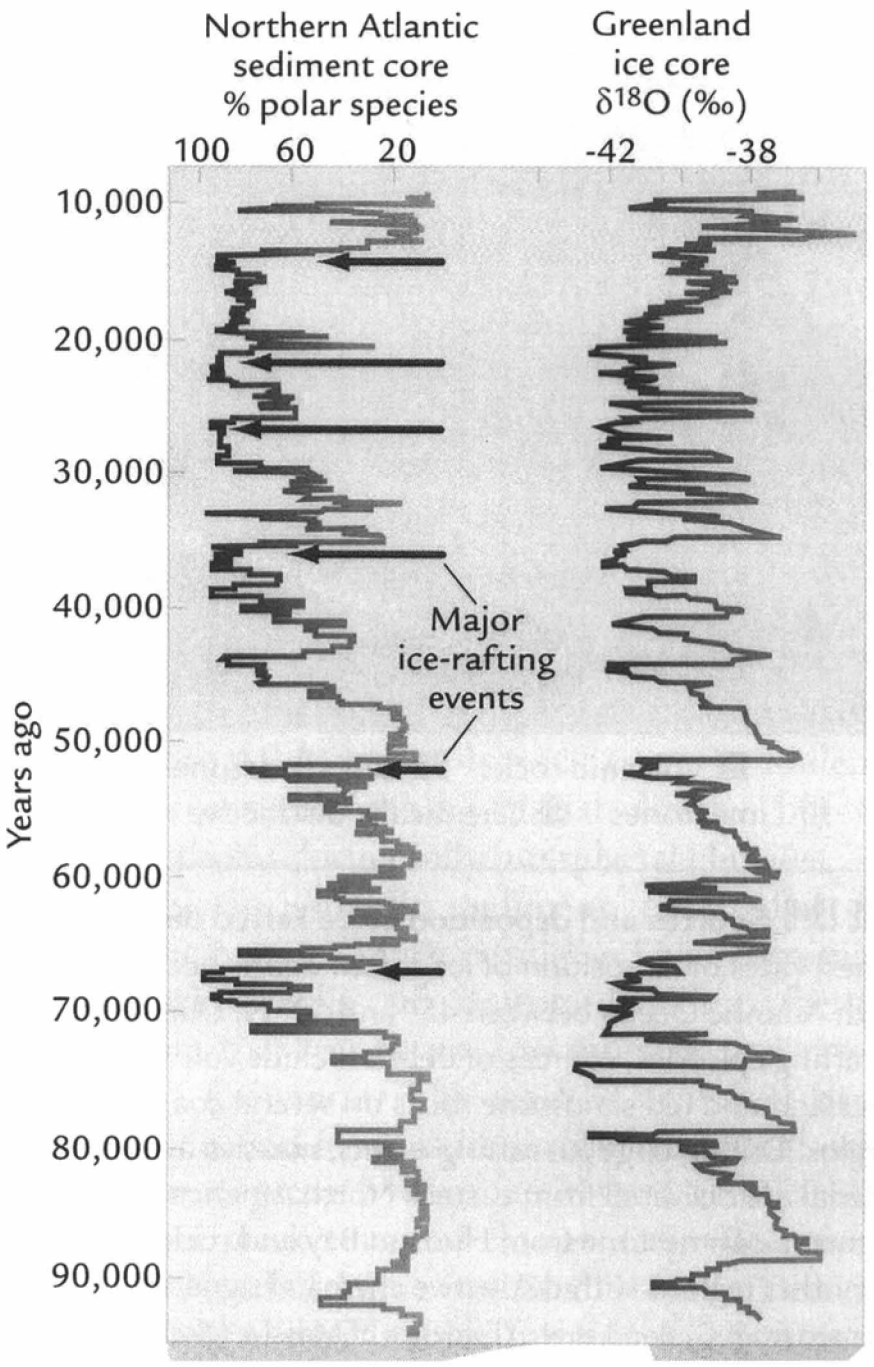

Figure 1. Diagram showing that millennial-scale fluctuations in composition of North Atlantic polar foraminifera and ice-rafted debris input (right) closely match $\delta^{18}O$ isotope changes in the Greenland ice cores (left); (Ruddiman, 2001).

1980's, the first continuous $\delta^{18}O$ isotope record (Figure 2) was constructed to about 2.75 million years ago (Mya). The record shows quasi-cyclic oscillations and a slow drift toward greater positive values. These features are a result of changes in temperature and ice volume. Positive $\delta^{18}O$ values indicate the presence of more ice and colder water temperatures. Negative $\delta^{18}O$ values indicate the presence of less ice and warmer water temperatures. Before 2.75 Mya, the $\delta^{18}O$ values appear to be relatively negative and no IRD was present in the subpolar North Atlantic; however, older IRD is present (but rare) off SE Greenland and in the Norwegian Sea. Consequently, either ice sheets did not exist around the North Atlantic or did not achieve the size necessary to calve icebergs. At 2.75 Mya, significant amounts of IRD appear for the first time in the sediment record. The accumulation of debris occurred mainly at 41,000 year cycles that may be in phase with $\delta^{18}O$ isotopes cycles; however, IRD and $\delta^{18}O$ isotope cycles may not be synchronous. This pattern is the likely response during small glaciations. Beginning near 0.9 Mya, there is a fundamental change in the $\delta^{18}O$ isotope record. The positive $\delta^{18}O$ values are higher than previously recorded and occur at 100,000 year intervals. This pattern is the likely response during large glaciations. There appear to be rapid decreases in the $\delta^{18}O$ values, which indicate rapid melting (deglaciation) (Ruddiman, 2001). During each 100,000 year cycle, the size and frequency of the IRD events were directly affected by the size of the ice sheet (McManus et al, 1999).

Sediment records from marine cores appear to correlate with isotope records from ice cores on land back to ~ 400,000 years; this correlation provides a more accurate view of abrupt climate change. When correlated with $\delta^{18}O$ data, the presence of IRD shows evidence for the periodic delivery of icebergs to the North Atlantic and changes in deep water circulation (Raymo et al, 1998). The close association of the onset and cessation of short-lived IRD events (i.e.,

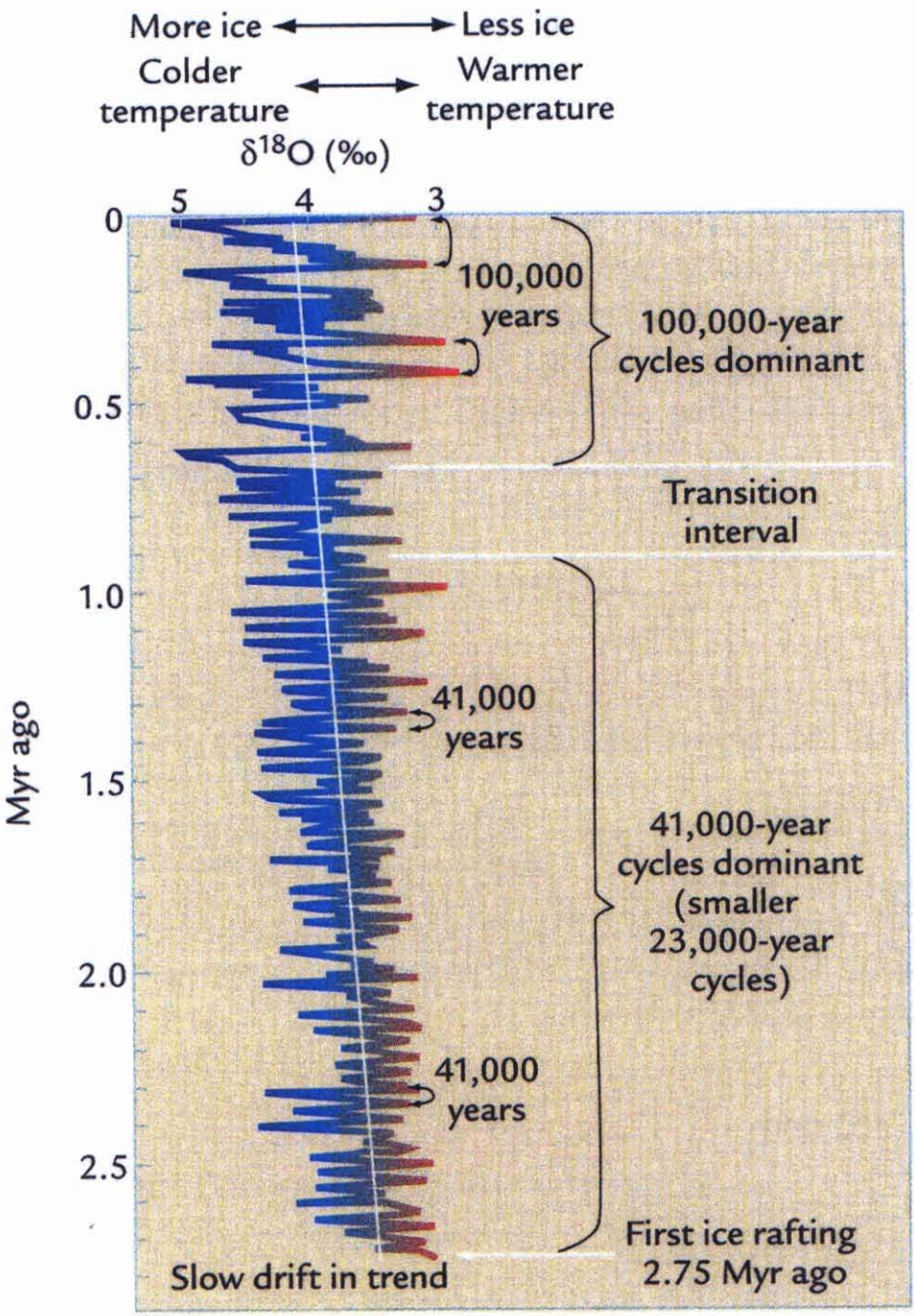

Figure 2. The full 2.75-Myr $\delta^{18}O$ record of the glacial history of the northern Hemisphere was compiled through the analysis of shells of benthic foraminifera, but also contained ice-rafted debris that directly marked times when ice sheets where present on adjacent continents. The diagram shows the transition from 41,000 year cycles to 100,000 year cycles at ~0.9 Mya. The diagonal white line shows the gradual long-term isotope trend toward more ice and colder climate conditions (Ruddiman, 2001)

Heinrich events, for example) with sudden changes in a benthic $\delta^{18}O$ proxy for ice volume records an important threshold in ice sheet growth and decay (i.e., evidence to support the "binge-purge" model) (McManus et al, 1999).

Significance of Ice-rafted Debris as a Climate Indicator for the North Atlantic

The ocean is by far the most effective location to retrieve older climate records, since on land such records are commonly destroyed by the passage of ice sheets. However, in the ocean sediment deposition is generally uninterrupted (Ruddiman, 2001). Two key indicators of past glaciation can be developed from ocean sediments:

1. the abundance of ice-rafted debris
2. $\delta^{18}O$ isotope records, which provide a measure of changes in ice volume and water temperature as preserved in the shells of foraminifera

Ice-rafted debris (IRD) can be defined as sediment that was transported by icebergs or sea ice in middle- and high- latitude marine settings, and that has settled to the sea floor as the icebergs melted (Krissek and St. John, 2002). IRD is a particularly useful marine proxy for understanding glacial activity on land. For example, deep marine IRD records have been used to document glacial expansion in the Northern Hemisphere during the Pliocene through the mid-Pleistocene, with specific focus on the Greenland Ice sheet (St. John and Krissek, 2002). The temporal distribution of IRD at a given site provides a history of glacial extension to sea level in that region; the geographic distribution and the composition of IRD aids in identifying the location of glaciated areas (Krissek and St. John, 2002) on both a regional and global scale.

The study of IRD in stratigraphically intact deep marine sediment sequences often

provides a relatively complete record of continental glaciation (Krissek and St. John, 2002). However, several factors have been found to affect the IRD record:

- the distribution and amount of sediment in the glacial ice
- the nature of the ice terminus
- the extent of offshore ice
- sea surface current patterns in the adjacent open ocean
- the presence or absence of sea ice in the open ocean
- sea surface temperature patterns which determine the location and rate of iceberg melting

Continuous marine deposits in a proximal offshore setting may potentially provide better long-term IRD records than more distal sites because (St. John and Krissek, 2002):

- IRD supply generally decreases further from the IRD source
- Mixing of IRD input from varying sources is more likely at greater distances from source
- Changes in iceberg dispersal due to changes in ocean currents are more likely as transport distance increases
- Changes in IRD melt-out due to sea surface temperature changes are more likely as transport distance increases
- Durability of the surficial material can affect long-distance transport

Advances and retreats in coastal glaciers over time are recorded through changes in the rate of IRD accumulation, measured either as an abundance (grains per gram of sediment, weight percent), or a mass accumulation rate ($g/cm^2/k.y.$). Although the rate of IRD accumulation is interpreted primarily as an indicator of glacial ice extent, it can also be affected by changes in the carrying capacity of the ice, the drift and melt patterns of the icebergs, the migration of

glaciomarine facies, and rate of iceberg supply. (St. John and Krissek, 2002; Krissek and St.John, 2002).

IRD has been deposited in the North Atlantic during both glacial and interglacial intervals; however, Figures 3 and 4 show that the abundance of IRD-rich deposits varies significantly from interglacials to glacials. During interglacial intervals, deposition resembled modern iceberg and sea ice distributions (Ruddiman, 1977). The amount of IRD generally was diminished during interglacial intervals due to the lack of sufficient continental ice at sea level around the North Atlantic where icebergs could calve (McManus et al, 1999). However, during glacial periods, the deposition of IRD increased, and was concentrated in zones at lower latitudes, where icebergs encountered warm water and melted (Ruddiman, 1977).

The axis of maximum IRD deposition, trending west-southwest along 46° - 50° N latitude, may mark the mean location of warm subpolar water during glacials (Fig. 4). This axis occurs along the southern limit of the polar front during moderate glacials, which lies about 5° to the north of, but parallel to, the position of the polar front during extreme full-glacial conditions (Ruddiman, 1977). The position of the Polar Front is important because it determines where icebergs will melt (Krissek and St. John, 2002).

The IRD pattern supplies a supplemental approach to reconstructing paleocirculation, as compared to micro -faunal and –floral estimates of paleotemperature and water movement (Ruddiman, 1977), because the deposition of IRD records the passage of melting icebergs. The pattern of deposition provides information about changes in past ocean circulation and about the size of the ice sheet on land. Dispersal patterns reveal more about the primary melting locus of the sediment-laden ice than about the trajectories of ice passage.

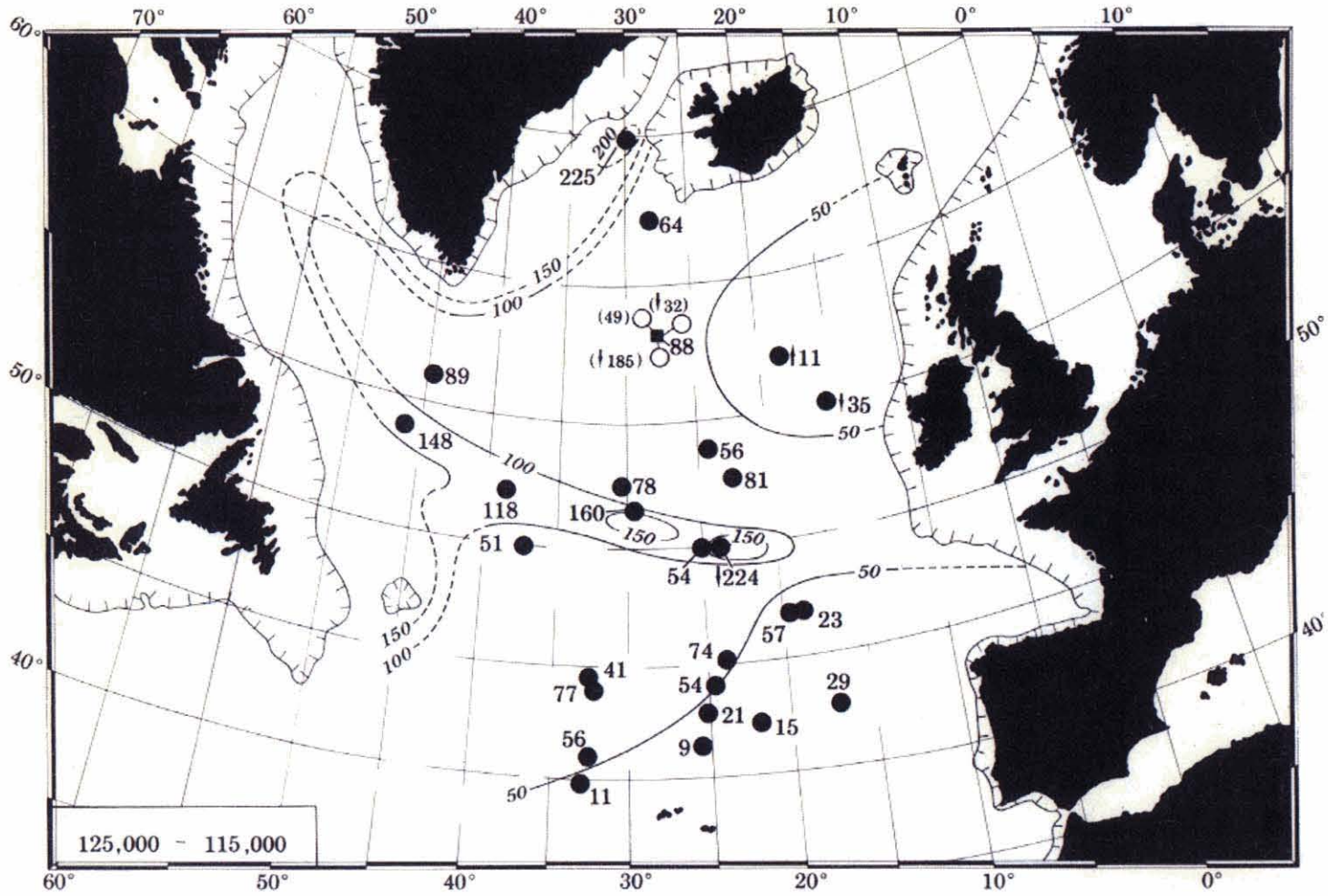

Figure 3. Mean rate of IRD deposition (mg / cm2 / 1000 years) in the North Atlantic during an interglacial period. This pattern largely resembles modern paths of sea ice/icebergs. (Ruddiman, 1977)

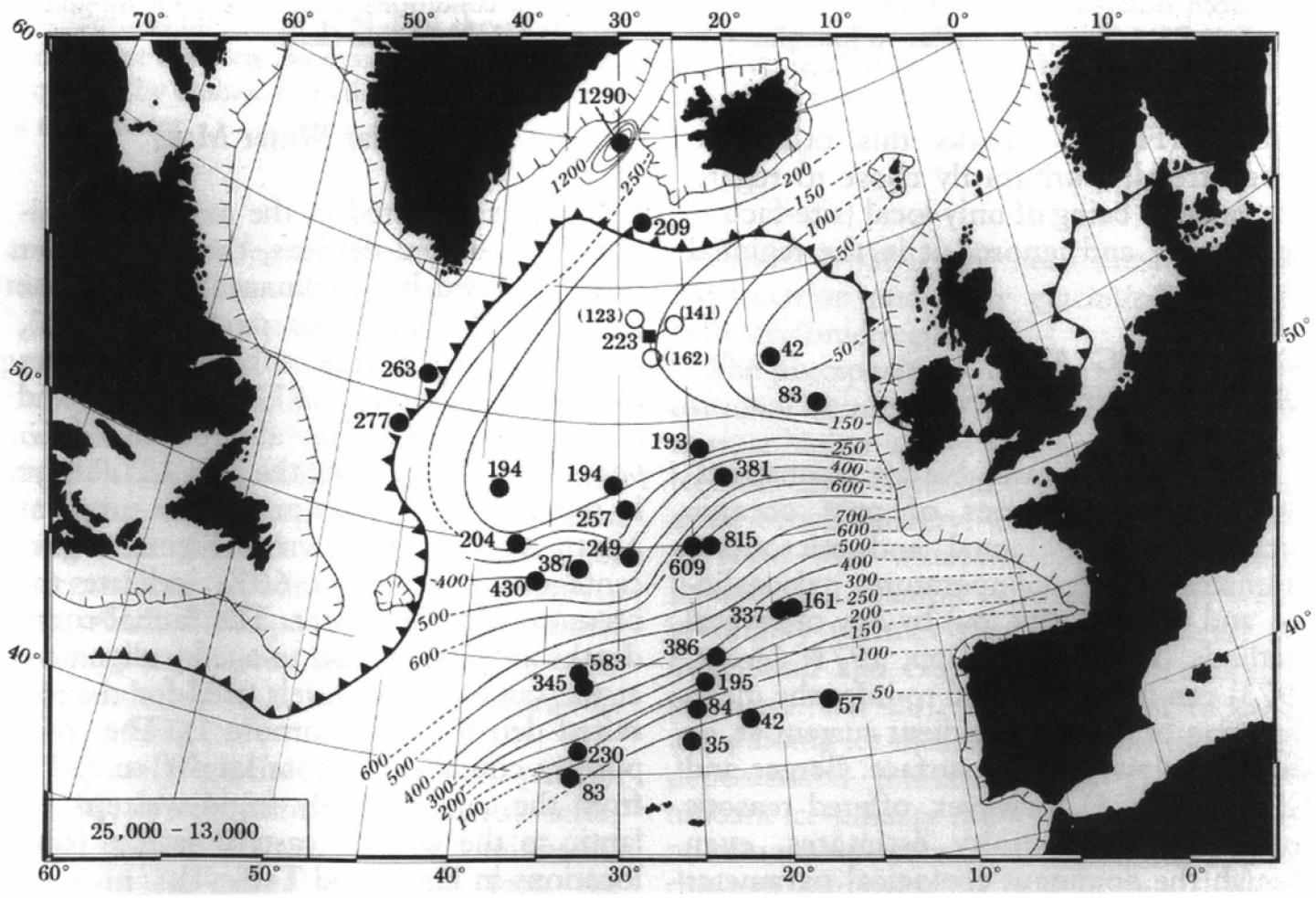

Figure 4. Mean rate of IRD deposition (mg / cm2 / 1000 years) in the North Atlantic during glacial period. Line with triangles is the ice-sheet limit on the continents and inferred ice limit over the ocean. (Ruddiman, 1977)

Milankovitch Theory and Influences on the North Atlantic

Over the years, there has been strong evidence from deep ocean sediments to link variations in climate with Milankovitch cycles (Figure 5). The Milankovitch theory identifies cyclic movements of the earth relative to the sun that combine to produce variations in the amount of solar radiation that is received by the earth's surface (Ahrens, 2003).

- Precession (23,000 years) describes the wobbling of the earth's axis of rotation
- Obliquity (41,000 years) describes changes in the tilt of the earth's axis.
- Eccentricity (100,000 years) describes changes in the shape of earth's orbit about the sun

Over the last 800,000 years, ice sheets have grown to a maximum approximately every 100,000 years. Previous studies provide evidence indicating that eccentricity appears to have been the dominant forcing factor on the frequency of glaciations during the last 800,000 years, controlling the severity of climatic variations. Prior to ~800,000 years ago, the dominant forcing factor appears to have been obliquity; the cause of this shift in behavior at ~800,000 years ago is still not well-understood.

Milankovitch cycles, in association with other natural factors, may help to explain the advance and retreat of ice over periods of 10,000 to 100,000 years (Ahrens, 2003). Orbital changes (i.e., Milankovitch cycles) alone are not totally responsible for the ice advance and retreat, but may provide a link between ice-sheet size and regional and global climate instability (McManus et al, 1999). Millennial-scale climate variations can be attributed to internal forcing mechanisms (i.e., ice-sheet dynamics, ocean-atmosphere interactions) and external forcings (i.e., solar radiation), or the combination of Milankovitch cycles (Raymo et al, 1998)).

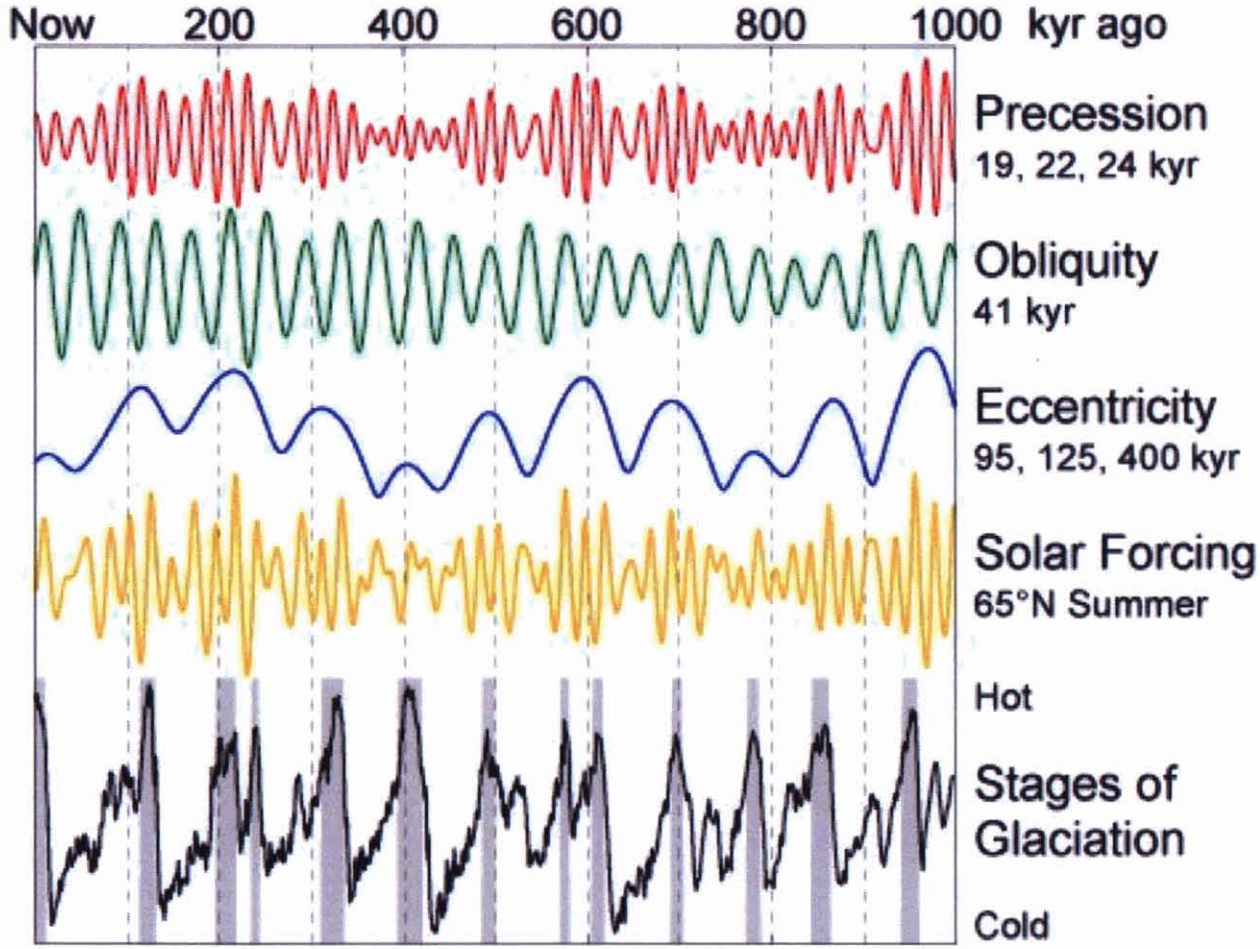

Figure 5. Diagram of the Milankovitch or "Orbital" cycles which show variations in insolation during the last one million years, with a resulting history of glaciations and interglacials. (en.wikipedia.org, 2006)

The Interplay of North Atlantic Climate and Thermohaline Circulation

Deep water circulation is driven by a sinking of cold water at higher latitudes and the subsurface movement of that cold water toward the equator. This overturning process is called the thermohaline circulation. Deep ocean water is one of the slowest-responding parts of the climate system. It takes about 1,000 years for the water that sinks to re-emerge at the surface (Ahrens, 2003). As Figure 6 illustrates, the thermohaline circulation, i.e. "salt conveyor", begins in the North Atlantic near Greenland and Iceland (Figure 7), where salty surface water is cooled through contact with cold Arctic air masses. The cold, dense water sinks and flows southward through the deep Atlantic Ocean, around Africa, and into the Pacific Ocean. Almost simultaneously, the sinking cool water draws warm surface water northward from the lower latitudes. As surface water flows, density variations (i.e., changes in temperature and salinity) result from the transfer of sensible and latent heat from the tropics to the polar regions, precipitation, and changes in the degree of runoff at the ocean surface (Bradley, 1999, p. 254). The thermohaline circulation appears to exhibit a bimodal behavior, which is controlled by changes in the amount of freshwater that is introduced into the North Atlantic Basin (Bradley, 1999, p. 257). A massive influx of freshwater into the system would cause the formation of an upper, low salinity water layer that would disrupt the movement of salty water in the North Atlantic and the conveyor would be "turned off". Ultimately, this would result in a reduction of heat transport into the North Atlantic and relatively colder climate conditions. During "conveyor off", the rate of salt transfer out of the North Atlantic is less than the rate of salt input due the level of evaporation. Salinity would gradually increase until a critical density threshold is met; at that point, the conveyor switches to "on" and there is an increase in saline water from the Gulf Stream. The ocean – atmosphere – cryosphere systems are in dynamic equilibrium, in which

disturbance of any one part of the system will ultimately lead to a nonlinear response in another system; and in doing so, the thermohaline circulation would be affected. Changes in deep water circulation are important for paleoclimatology because large quantities of heat are carried around the globe as a result of deep water formation and compensating fluxes of freshwater in the upper mixed layers of the ocean (Bradley, 1999, p. 257). Variations in deep water circulation play a critical role in driving and amplifying millennial-scale climate oscillations (Oppo et al, 1998).

Heinrich Events and Their Effect on Thermohaline Circulation

The near-global footprint of Heinrich events is a testament to the interactions between the ocean, atmosphere, and cryosphere (Hemming, 2004). Within the last glacial cycle, six intervals have been identified in sediment cores as the records of Heinrich events. Heinrich events are episodes of very rapidly accumulating ice-rafted debris (IRD) at times associated with a drop in foraminifera concentrations, due to lower production or increased dissolution (Bradley, 1999, p. 262). Heinrich layers are IRD-rich deposits in the North Atlantic, interpreted to have resulted from massive discharges of icebergs from the Laurentide Ice Sheet through the Hudson Strait. The Hudson Strait is a major trough and most likely was the location of an ice stream capable of draining the eastern part of the Laurentide Ice Sheet (Hemming, 2004). There have been numerous episodes when a massive draw-down of ice in one or more circum-Atlantic ice sheets resulted in "armadas of icebergs" and entrained basal debris entering the cold waters of the North Atlantic (Bradley, 1999, p. 266). The presence of large continental ice sheets in the Northern Hemisphere may have led to increased climate instability (Hemming, 2004).

The Heinrich events are clearly linked to dramatic climate shifts in the Northern

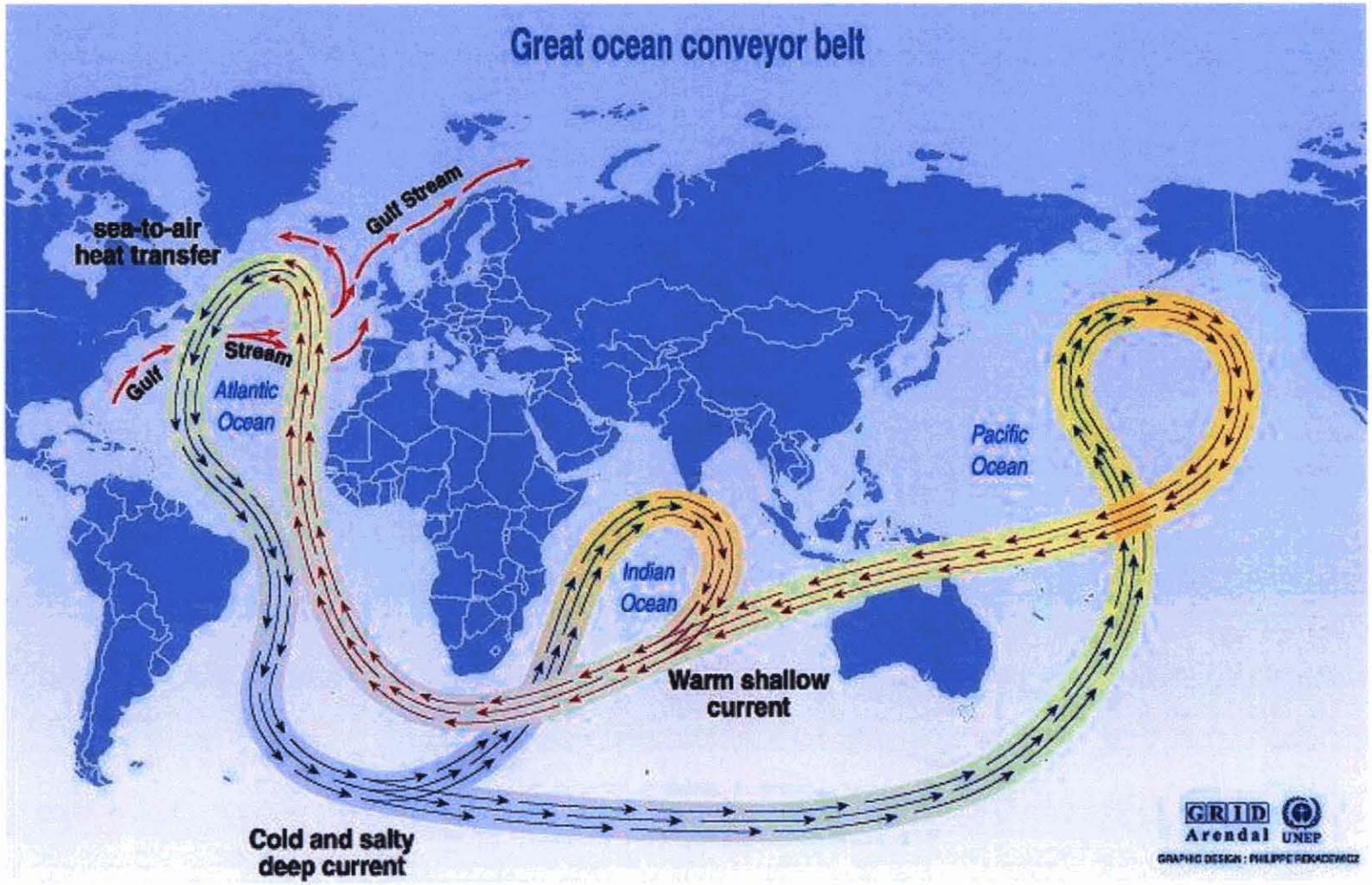

Source: Broecker, 1991, in Climate change 1995, impacts, adaptations and mitigation of climate change: scientific-technical analyses, contribution of working group 2 to the second assessment report of the intergovernmental panel on climate change, UNEP and WMO, Cambridge press university, 1996.

Figure 6. Diagram of the Global Thermohaline Circulation

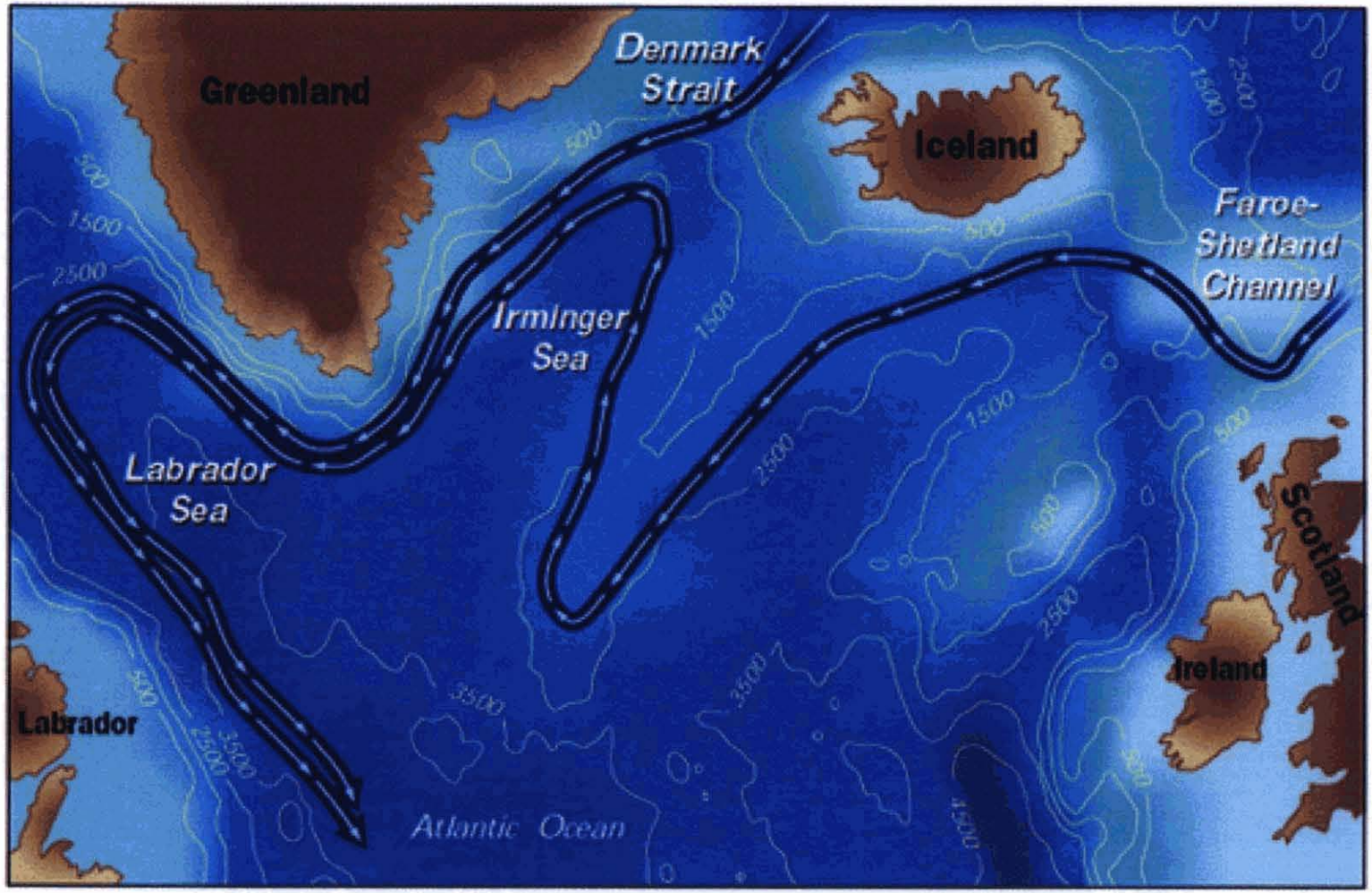

Figure 7. Regional snapshot of the Thermohaline Circulation in the Northern Hemisphere in the North Atlantic (Gagosian, 2003: www.whoi.edu)

Hemisphere, and they have global correlations (Hemming, 2004). Heinrich events generally occur at the end of prolonged cooling episodes, indicating a possible link between the ocean and atmospheric systems, and changes in ice-sheet dynamics (Bradley, 1999, p. 263). Heinrich events appear to have occurred when climate conditions were already cold and much of the North Atlantic was covered by cold polar waters. One explanation for their occurrence is the "binge-purge" model (Bradley, 1999, p. 267). The premise of the "binge-purge" model is that a large ice sheet will build up gradually during a binge phase, dependent on air temperature and moisture supply. Once the ice sheet reaches a critical thickness, basal melting is proposed to destabilize the ice sheet, resulting in a rapid discharge or purge phase (Hemming, 2004). For the Heinrich events, this rapid discharge is commonly interpreted to have been produced by the collapse of the ice sheet into the Hudson Strait. However, the conditions necessary for such a destabilization are still not well understood. There appears to be a delicate balance between the conditions that maintain an ice sheet in a quasi-equilibrium state, those that cause a periodic collapse followed by recovery, and those that trigger an irreversible collapse (complete deglaciation). There is evidence to suggest that Heinrich events themselves may be a direct consequence of changes in ocean and atmospheric circulations in low latitudes due to orbital forcing (Bradley, 1999, p. 267).

3. Study Region and Site Description

IODP Expedition 303

The primary objective of Expedition 303 was to develop late Neogene – Quaternary climatic proxies for the North Atlantic and to place these proxies into a paleointensity – assisted chronology (PAC). A PAC is based on data collected from geomagnetics, stable isotopes, and detrital layers. Expedition 303 selected drill sites with the potential to yield complete, continuous sediment records displaying millennial-scale environmental variability (i.e., ice-sheet/ocean interactions, deep water circulation, and sea-surface conditions) and suitable for the development of high-resolution stratigraphies. The integrated stratigraphy (Figure 8) will allow the climate record to be placed in a suitable framework for correlating North Atlantic climate records, from previous studies and other sites, and to high-resolution records established elsewhere (Channell et al, 2005).

Site 1305

Site 1305 (Figure 9) was the designated deep water site (3459 m deep water) at the southwestern end of the Eirik Drift, off the southeastern coast of Greenland. This site is located under the Western Boundary Undercurrent (WBUC), which strongly affected sedimentation during the last glacial cycle. A composite section was constructed by drilling three holes with an advanced piston corer (APC) to about 295 meters composite depth (mcd). The record at Site 1305 does not display any significant time gaps; however, it does contain relatively expanded interglacial intervals and condensed glacial intervals. The mean sedimentation rate is 17 cm / ky, which promises a high resolution record of ice sheet instability and changes in surface and deep water masses. Sites with high sedimentation rates, such as Site 1305, permit the study of

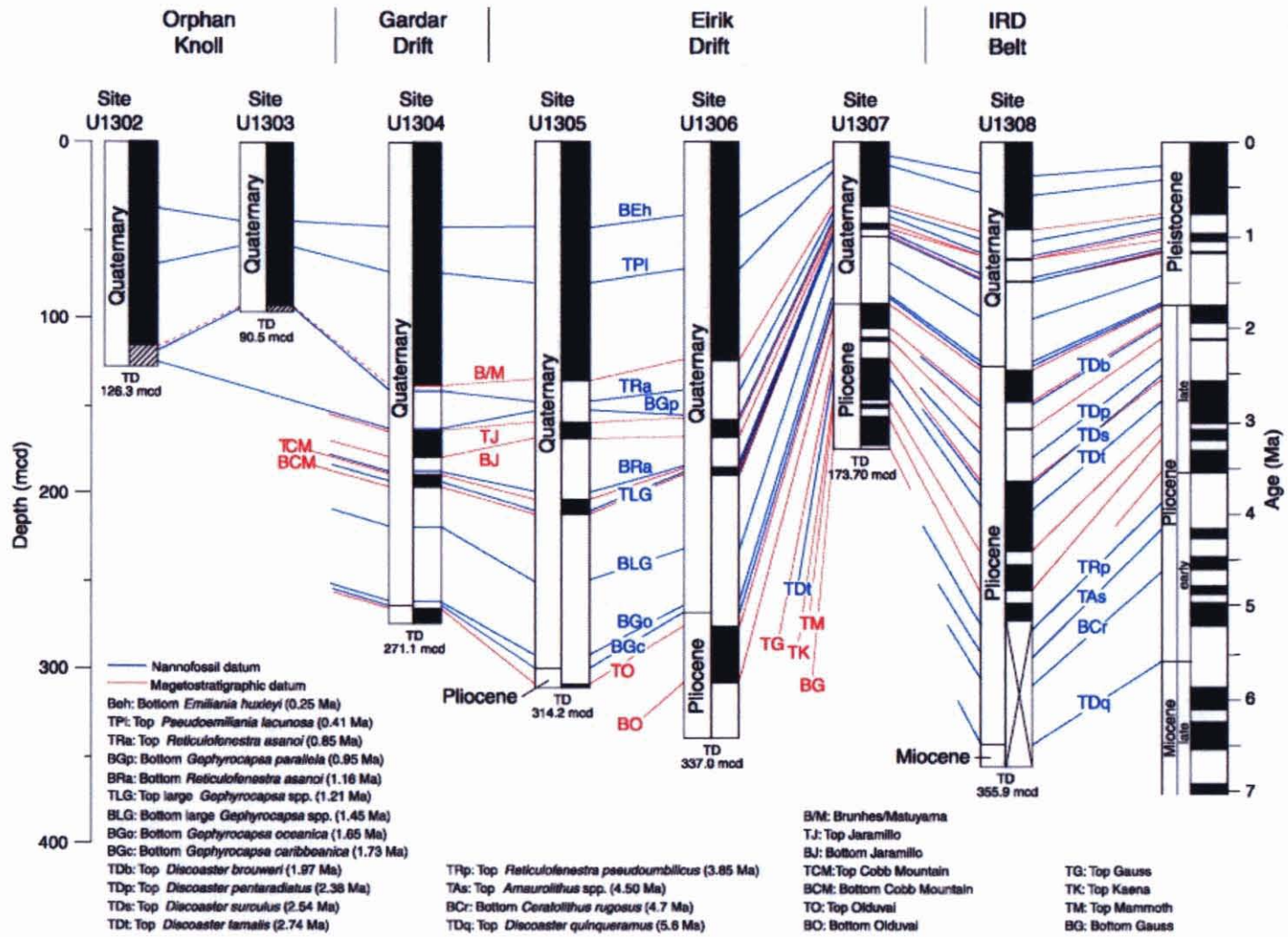

Figure 8. Schematic stratigraphy at the seven sites drilled during Expedition 303. At Site 1305, three cores were drilled to yield a complete and continuous sediment record at this location. Note there are no significant time gaps within the record at Site 1305. (Channell et al, 2005)

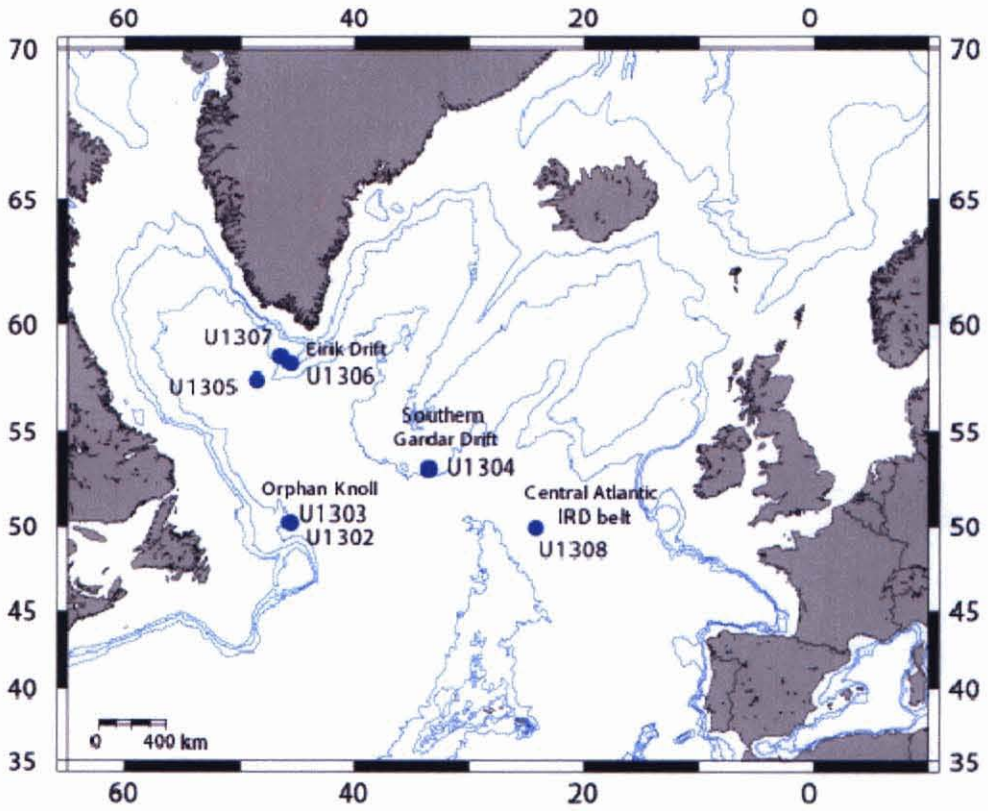

Figure 9. Map of IODP Expedition 303 Sites. Note the location of Site 1305 which will be examined in this study. (Channell et al, 2005)

millennial scale climate variability.

4. Methods

The objective of this study was to determine the IRD input history at Site 1305, using approximately 380 samples, with an estimated spacing of ~3,000 -4,000 years between samples. However, due to time constraints, only ~200 samples have been analyzed at the present time. These samples were analyzed to determine the abundance of ice-rafted debris (IRD). Various definitions for IRD have been proposed in past studies; for this study, IRD is defined as the lithic grains in the >150 μm fraction. The abundance of IRD was determined as the weight percent of the >150 μm fraction relative to the total sediment present. Each sample weighed between 6 and 21 grams. To obtain data, each sample was placed into a small pan and dried, for approximately 24 hours in an oven at 85 ° C. Each sample was then weighed. If necessary, samples were placed in a sonic bath to help break down the sample to make it easier to sieve. Each sample then was wet-sieved at 150 μm and 2mm. Each washed residue was dried, for approximately 6 hours, and reweighed. Finally, each sample was placed in a small, labeled vial for storage. The sample ages were determined using an age-depth model developed by the Expedition 303 Scientific Party. Future study will include examining the sieved residues with a binocular microscope to determine the number of lithic grains and the abundances of various grain types. The grain composition will be used to determine the source region(s) and possible trajectory of the icebergs.

5. Results

There are variations in the abundances of ice-rafted debris at Site 1305. For the samples

analyzed, the abundance of the > 150 μm sand fraction ranged of 0.02 to 13.37 weight percent (wt %). For the samples analyzed, the abundance of the > 2 mm grand fraction ranged from 0.03 to 5.31 wt %. Figure 10 displays the IRD weight percents of the > 150 μm fraction plotted versus age (k.y.). The age calculations were made based on linear extrapolation between magnetostratigraphic and biostratigraphic age-depth data collected during Expedition 303.

There are a series of large IRD maxima distributed throughout the last one million years at Site 1305. The oldest peak in IRD abundance occurs at a depth of 128.42 meters below sea floor (mbsf), which has a calculated age of 833.5 thousand years ago (kya) and a 7.49 wt%. This is followed by a series of relatively large peaks at ~563.8 kya (6.45 wt %), ~287 kya (13.37 wt%), and ~62.5 kya (7.32 wt%).

In the 2 to 4.5 wt % range, there are several significant IRD peaks distributed throughout the record. These series of peaks in IRD abundance occur at: ~82.5 kya (4.01 wt %), ~304 kya (3.57 wt %), ~635.2 kya (3.26 wt %), ~353.5 kya (3.12 wt %), and ~364.97 kya (3.04 wt %).

In the 0.87 to 2 wt % range, there are several significant IRD peaks distributed throughout the record. This series of peaks in IRD abundance occur at: ~648.4 kya (1.67 wt %), ~182.5 kya (1.65 wt %), ~ 468.3 kya (1.54 wt %), ~ 629.5 kya (1.50 wt %), and ~295.6 kya (1.16 wt %).

With the exception of these significantly large peaks, the large majority of the data appears to fall below the overall average value of 0.87 wt %.

For the IRD maxima that are greater than 2 wt %, Table 1 shows the in timing of the IRD maxima relative to the isotope stage boundaries. When the IRD peaks occurs after the stage boundary, the lags range from 2.9 to 9.5 ky. When the IRD peak occurs before the stage boundary, the lead time ranges from 18.5 to 62.8 ky.

Glacial Stage	Boundary Age (ky)	Peak Age (ky)	Lag By (ky)
18	700	697.1	2.9
12	476	468.3	7.7
10	360	353.5	6.5
6	192	182.5	9.5

Glacial Stage	Boundary Age (ky)	Peak Age (ky)	Leads By (ky)
16	606	635.2	29.2
14	501	563.8	62.8
8	268	287	19
4	64	82.5	18.5

Table 1. Age of Peak IRD maxima relative to onset of glaciation

The majority of the large peaks in this record include at least one data point intermediate between the maximum and minimum values, suggesting that these fluctuations are not just a result of the sample interval. Since not all the samples have been processed, however, it must be acknowledged that some of the fluctuations in the IRD abundances are likely to be missing from this record. The original estimate of a sample spacing of ~3,000-4,000 years is not correct because not all the samples have been analyzed; based on the analyzed samples, the actual sample spacing is ~6,000-8,000 years.

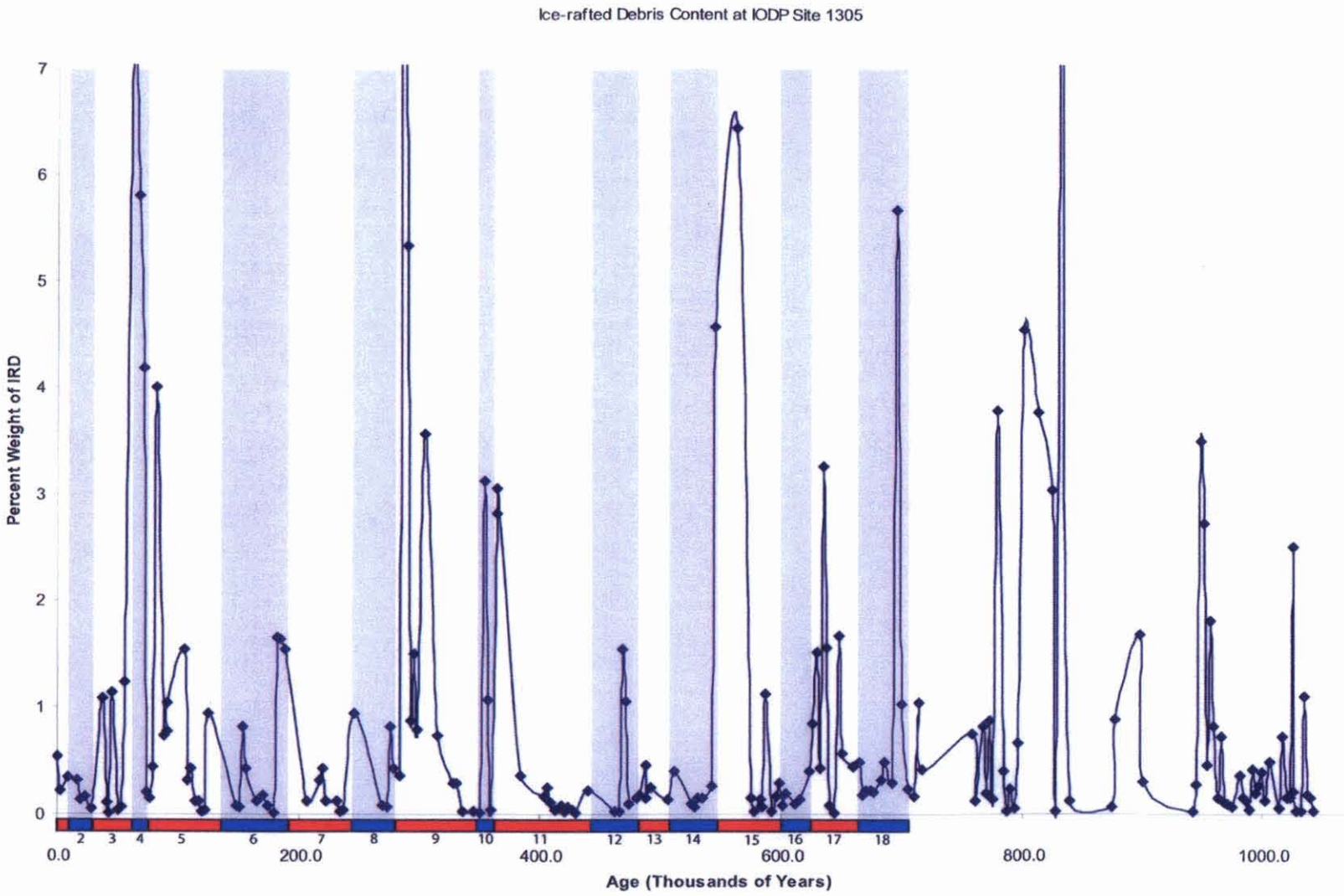

Figure 10. Plot age versus IRD weight percentage for the cores drilled at Site 1305. Glacial (blue) and interglacial (red) stage boundaries have been identified at bottom of chart. $\delta^{18}O$ isotope stages 1-18 are represented by shaded and unshaded horizontal bars and are numbered along the bar. Note that the vertical axis has been truncated at 7 wt % to give a more accurate depiction of curve below that percentage.

6. Discussion

The North Atlantic appears to be prone to periods of abrupt climate changes on various time-scales; however, the mechanisms and causes of such episodes of change are still not widely understood. $\delta^{18}O$ isotope records from the North Atlantic appear to indicate a long-term trend of a slow drift from warmer temperatures (less ice) to colder temperature (more ice) toward the present; however, the sediment record from Site 1305 does not appear to show any similar long-term trends in IRD supply over the last one million years.

The series of large IRD maxima, which are distributed throughout the record, appear to have a quasi-cyclic pattern that repeats approximately every 100,000 years (± 1,500 years). As Figure 10 illustrates, the major IRD peaks do not lie in the middle of a glacial or interglacial, nor do most of them straddle glacial/interglacial transitions. Instead, most of the IRD maxima occur just before or just after the onset of glaciation. A few IRD maxima are positioned at the height of a glacial stage. Although, one might assume that IRD abundances would be low near the end of an interglacial cycle. The data from Site 1305 provides evidence that ice-rafting increased during the early stages of global ice increase from sources affecting Site 1305. In other words, controls acting on a local, not global, level were having more of an effect on ice production and the transport and melting of icebergs in the region of the Eirik Drift, off the southeastern coast of Greenland.

It is also interesting to note that transitions into stages 16, 12, 10, 8, and 6, all of which appear to have relatively high IRD peaks (either slightly before or during the onset of glaciation), are marked by relatively large amplitude changes in the benthic oxygen isotope record (Bradley, 1999, fig 6.11);(Krissek and St. John, 2002). These isotope shifts suggest drastic changes in climate, from periods with climates suitable for extensive weathering to relatively intense

glaciations. As a result of these climate changes, advancing glaciers could have moved across a surface of weathered and easily eroded materials. Once this weathered veneer was removed, the rate of IRD supply could decrease as shown by IRD abundances that decrease significantly late in the glacial stage and into the onset of deglaciation. Another possible control on this timing of maximum IRD input is variations in the amount of sea ice. Sea ice may have been scarce coming into a glacial, so that IRD-bearing icebergs could move offshore. Later, during full glacial conditions, more extensive sea ice may have limited iceberg movement and IRD dispersal to Site 1305.

7. Conclusions

Previous studies of IRD abundances have been instrumental in developing marine records of millennial-scale climate variations. This study will contribute to developing a millennial-scale record of sediments deposited in the North Atlantic by icebergs. From the data provided by the samples analyzed at Site 1305, the following conclusions can be made:

- The sediment record at Site 1305 provides no evidence of any long term trends in the IRD supply during the last one million years
- There is evidence to support an apparent 100,000 year cyclicity in IRD input
- IRD maxima often recur just before or just after the boundary at the start of a glacial stage. This position may be the result of
    - differences in the origin of the two signals (local for IRD; global for ice volume)
    - a transition from easily eroded to more competent surface materials as ice volume increased

- and changes in the volume and presence of sea ice

Further work should focus on: 1) analyzing the remainder of the existing samples, 2) filling in gaps in the data set in order to observe shorter period (sub-Milankovitch) cycles; 3) examining the grain composition of the samples to identify iceberg sources. By identifying the grain composition, the controls (local, regional, and global) acting in the source(s) of the IRD may be better understood.

References

Arhens, C. D. 2003. Meterology Today: An Introduction to Weather, Climate, and the Environment. Thomson Learning Brook/Cole: CA. Seventh Ed. ch 19. pp. 522-531.

Bradley, R.S. 1999. Paleoclimatology: Reconstructing Climates of the Quaternary. Harcourt/Academic Press: Burlington, MA. Second ed. pp. 254-283.

Channell, J.E.T, et al. 2006. IODP Expeditions 303 and 306 Monitor Miocene-Quaternary Climate in the North Atlantic. Scientific Drilling. no 2. pp 4-10. doi:10.2204/iodp.sd.2.01.2006

Hemming, S. K. 2004. Heinrich Events: Massive late Pleistocene detritus layers of the North Atlantic and their global climate imprint. Review of Geophysics, 42.

Krissek, L. A., St. John, K. E. K. 2002. Pleistocene iceberg production from East Greenland: Synchronous between source areas, but distinct from glacial ice volume. Bulletin of the Geological Society of Denmark, vol. 49, pp. 77-89. Copenhagen.

McManus, J.F., Oppo, D.W., Cullen, J.L. 1999. A 0.5-million year record of Millennial-scale climate variability in the North Atlantic. Science. Vol. 283. pp. 971-974.

Oppo, D.W., McManus, J.F., Cullen, J.L. 1998. Abrupt Climate Events 500,000 to 340,000 years ago: Evidence for Subpolar North Atlantic Sediments. Science, vol. 279. pp. 1335-1338.

Raymo, M. E., Ganley, K., Carter, S., Oppo, D. W., McManus, J. 1998. Millennial-scale climate instability during the early Pleistocene epoch. Nature, vol, 392, pp. 699-702.

Ruddiman, W.F. 1977. Late Quaternary deposition of ice-rafted sand in the subpolar North Atlantic (Lat 40°N to 65°N). Geol. Sci. Am. Bull., vol 88, pp. 1813-1827.

Ruddiman, W.F. 2001. Earth's Climate: Past and Future. W.H. Freeman and Company: New York, NY. pp. 220-228, 255-273, 331-337

St. John, K. E. K., Krissek, L. A. 2002. The last Miocene to Pleistocene ice-rafting history of southeast Greenland. Boreas, vol 31, pp. 28-35. Oslo.

Appendix

Ice-rafted Debris Content at IODP Site 1305

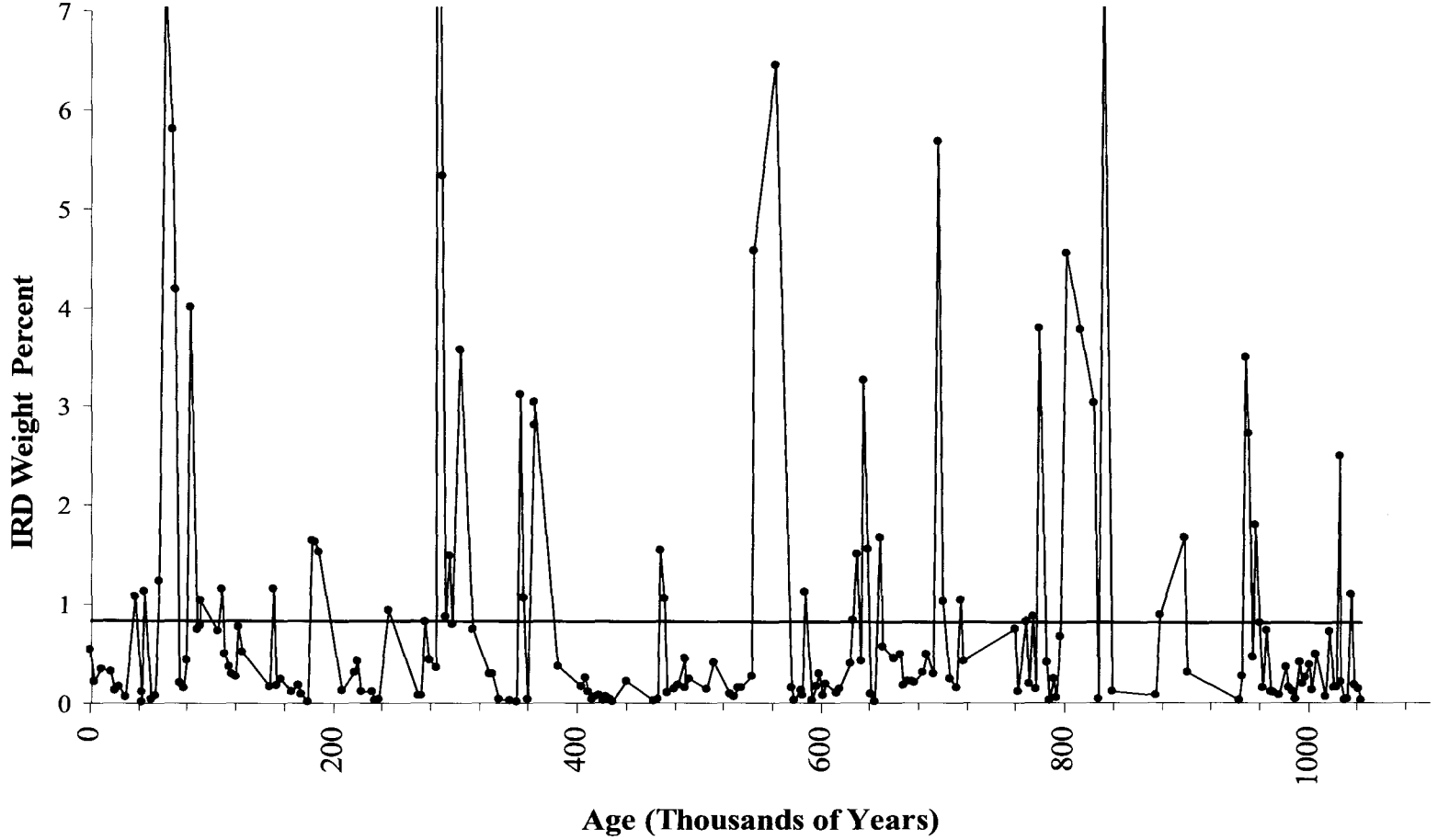

* Vertical line through data points shows the overall IRD abundance value of 0.84 wt%.

Hole	Core	Section	Top of Interval (cm)	Depth (mbsf)	Depth (mcd)	Age (kya)	Bulk Dry Weight (grams)	Dry Weight (> 150 µm)	Dry Weight (> 2 mm)	IRD wt% (> 150 µm)	IRD wt % (> 2 mm)
A	1	3	52	3.52	7.4	42.3	17.403	0.0190		0.11	
A	1	3	102	4.02	7.9	45.1	9.680	0.1100		1.14	
A	1	4	52	5.02	8.9	50.9	12.003	0.0050		0.04	
A	1	4	102	5.52	9.4	53.7	12.205	0.0090		0.07	
A	1	5	2	6.02	9.9	56.6	13.482	0.1660		1.23	
A	2	2	102	11.42	15.94	91.1	9.005	0.0700		0.78	
A	2	4	52	13.92	18.44	105.4	7.823	0.0570	0.0640	0.73	0.82
A	2	4	102	14.42	18.94	108.2	7.753	0.0900		1.16	
A	2	5	2	14.92	19.44	111.1	7.103	0.0360		0.51	
A	2	5	52	15.42	19.94	113.9	11.356	0.0430		0.38	
A	2	5	102	15.92	20.44	116.8	12.211	0.0360		0.29	
A	2	6	2	16.42	20.94	119.7	10.154	0.0280		0.28	
A	2	6	52	16.92	21.44	122.5	9.527	0.0740	0.0430	0.78	0.45
A	2	6	102	17.42	21.94	125.4	9.399	0.0480	0.0190	0.51	0.20
A	3	2	52	20.42	25.93	148.2	11.632	0.0200		0.17	
A	3	2	102	20.92	26.43	151.0	13.396	0.1540	0.0040	1.15	0.03
A	3	3	2	21.42	26.93	153.9	5.391	0.0100		0.19	
A	3	3	52	21.92	27.43	156.7	14.725	0.0350		0.24	
A	3	4	52	23.42	28.93	165.3	15.222	0.0180		0.12	
A	3	5	2	24.42	29.93	171.0	15.876	0.0290		0.18	
A	3	5	52	24.92	30.43	173.9	12.501	0.0110		0.09	
A	3	6	2	25.92	31.43	179.6	12.791	0.0010		0.01	
A	3	6	52	26.42	31.93	182.5	11.700	0.1930		1.65	
A	3	6	102	26.92	32.43	185.3	7.092	0.1160	0.0460	1.64	0.65
A	3	7	2	27.42	32.93	188.2	9.722	0.1490	0.0150	1.53	0.15
A	4	3	52	31.42	38	217.1	11.803	0.0370		0.31	
A	4	3	102	31.92	38.5	220.0	10.643	0.0450		0.42	

A	4	4	2	32.42	39	222.9	11.023	0.0130		0.12	
A	4	5	2	33.92	40.5	231.4	7.510	0.0090		0.12	
A	4	5	52	34.42	41	234.3	11.280	0.0030		0.03	
A	4	5	102	34.92	41.5	237.1	9.383	0.0040		0.04	
A	4	6	102	36.42	43	245.7	14.517	0.1360	0.0880	0.94	0.61
A	5	2	102	39.92	47.23	269.9	17.216	0.0140		0.08	
A	5	3	2	40.42	47.73	272.7	10.966	0.0080		0.07	
A	5	3	52	40.92	48.23	275.6	12.881	0.1060		0.82	
A	5	3	102	41.42	48.73	278.5	10.574	0.0460		0.44	
A	5	4	52	42.42	49.73	284.2	13.508	0.0480		0.36	
A	5	4	102	42.92	50.23	287.0	21.485	2.8720	0.5440	13.37	2.53
A	5	5	2	43.42	50.73	289.9	9.992	0.5330	0.0760	5.33	0.76
A	5	5	52	43.92	51.23	292.7	9.288	0.0810		0.87	
A	5	5	102	44.42	51.73	295.6	11.132	0.1660		1.49	
A	5	6	2	44.92	52.23	298.5	9.834	0.0780		0.79	
A	5	6	102	45.92	53.23	304.2	10.712	0.3820		3.57	
A	6	2	52	48.92	57.86	330.6	10.748	0.0320		0.30	
A	6	3	2	49.92	58.86	336.3	12.428	0.0040		0.03	
A	6	4	2	51.42	60.36	344.9	14.544	0.0040		0.03	
A	6	4	102	52.42	61.36	350.6	16.444	0.0030		0.02	
A	6	5	2	52.92	61.86	353.5	14.716	0.4590	0.0690	3.12	0.47
A	6	5	52	53.42	62.36	356.3	8.613	0.0920		1.07	
A	6	5	102	53.92	62.86	359.2	10.740	0.0040		0.04	
A	6	6	52	54.92	63.86	364.9	8.232	0.2320		2.82	
A	7	3	102	60.42	70.61	403.5	11.525	0.0190		0.16	
A	7	4	2	60.92	71.11	406.3	14.210	0.0360		0.25	
A	7	4	52	61.42	71.61	409.2	16.155	0.0180		0.11	
A	7	4	102	61.92	72.11	412.1	10.579	0.0040		0.04	
A	7	5	2	62.42	72.61	414.9	12.894	0.0080		0.06	

A	7	5	52	62.92	73.11	417.8	16.950	0.0130		0.08	
A	7	5	102	63.42	73.61	420.6	12.560	0.0030		0.02	
A	7	6	2	63.92	74.11	423.5	15.653	0.0100		0.06	
A	7	6	52	64.42	74.61	426.3	16.715	0.0070		0.04	
A	7	6	102	64.92	75.11	429.2	13.213	0.0020		0.02	
A	8	3	52	69.42	80.95	462.6	12.140	0.0030		0.02	
A	8	3	102	69.92	81.45	465.4	15.363	0.0050	0.8150	0.03	5.30
A	8	4	2	70.42	81.95	468.3	10.673	0.1640		1.54	
A	8	4	52	70.92	82.45	471.1	12.596	0.1330	0.0190	1.06	0.15
A	8	4	102	71.42	82.95	474.0	14.526	0.0150		0.10	
A	8	5	52	72.42	83.95	479.7	14.935	0.0220		0.15	
A	8	5	102	72.92	84.45	482.6	16.349	0.0300		0.18	
A	8	6	52	73.92	85.45	488.3	15.654	0.0710		0.45	
A	9	3	102	79.42	92.02	525.8	9.759	0.0090		0.09	
A	9	4	2	79.92	92.52	528.7	18.355	0.0120		0.07	
A	9	4	52	80.42	93.02	531.5	14.655	0.0220		0.15	
A	9	4	102	80.92	93.52	534.4	15.204	0.0240		0.16	
A	9	5	102	82.42	95.02	543.0	13.623	0.0360		0.26	
A	9	6	2	82.92	95.52	545.8	12.095	0.5530	0.0970	4.57	0.80
A	10	3	52	88.42	102.24	584.2	14.479	0.0110		0.08	
A	10	3	102	88.92	102.74	587.1	10.979	0.1230		1.12	
A	10	4	52	89.92	103.74	592.8	12.531	0.0040		0.03	
A	10	4	102	90.42	104.24	595.7	16.500	0.0280		0.17	
A	10	5	2	90.92	104.74	598.5	16.509	0.0490		0.30	
A	10	5	52	91.42	105.24	601.4	12.859	0.0100		0.08	
A	10	5	102	91.92	105.74	604.2	14.134	0.0270		0.19	
A	12	2	102	106.42	121.99	697.1	12.142	0.6890	0.1370	5.67	1.13
A	12	3	2	106.92	122.49	699.9	11.253	0.1160	0.1010	1.03	0.90
A	12	3	102	107.92	123.49	705.7	13.268	0.0320		0.24	

A	12	4	52	108.92	124.49	711.4	14.960	0.0240		0.16	
A	12	4	102	109.42	124.99	714.2	13.760	0.1440		1.05	
A	12	5	2	109.92	125.49	717.1	18.450	0.0780		0.42	
A	14	2	52	124.92	142.36	813.5	16.190	0.6110	0.0620	3.77	0.38
A	14	3	102	126.92	144.36	824.9	14.415	0.4370	0.0650	3.03	0.45
A	14	4	2	127.42	144.86	827.8	15.280	0.0050		0.03	
A	14	4	102	128.42	145.86	833.5	17.698	1.3260	1.0560	7.49	5.97
A	14	5	52	129.42	146.86	839.2	14.039	0.0170	0.0250	0.12	0.18
A	15	2	102	134.92	153.13	875.0	11.122	0.0080		0.07	
A	15	3	2	135.42	153.63	877.9	9.386	0.0830		0.88	
A	15	5	52	138.92	157.13	897.9	10.714	0.1790	0.3830	1.67	3.57
A	15	5	102	139.42	157.63	900.7	12.955	0.0400		0.31	
A	16	3	102	145.92	164.98	942.7	17.503	0.0050		0.03	
A	16	4	2	146.42	165.48	945.6	9.208	0.0250		0.27	
A	16	4	52	146.92	165.98	948.5	10.638	0.3720	0.0670	3.50	0.63
A	16	4	102	147.42	166.48	951.3	9.712	0.2640	0.0440	2.72	0.45
A	16	5	2	147.92	166.98	954.2	13.148	0.0610		0.46	
A	16	5	52	148.42	167.48	957.0	17.072	0.3080		1.80	
A	16	5	102	148.92	167.98	959.9	13.897	0.1130		0.81	
A	16	6	2	149.42	168.48	962.7	12.741	0.0200		0.16	
A	16	6	52	149.92	168.98	965.6	15.703	0.1140		0.73	
A	16	6	102	150.42	169.48	968.5	17.362	0.0200		0.12	
A	16	7	2	150.92	169.98	971.3	13.722	0.0140		0.10	
A	17	3	2	154.42	174	994.3	13.309	0.0250		0.19	
A	17	3	52	154.92	174.5	997.1	10.648	0.0280	0.0620	0.26	0.58
A	17	3	102	155.42	175	1000.0	12.209	0.0470		0.38	
A	17	4	2	155.92	175.5	1002.9	10.970	0.0140		0.13	
A	17	4	52	156.42	176	1005.7	16.341	0.0790		0.48	
A	17	5	52	157.92	177.5	1014.3	13.368	0.0080		0.06	

A	17	5	102	158.42	178	1017.1	14.669	0.1050		0.72	
A	17	6	2	158.92	178.5	1020.0	12.118	0.0190		0.16	
A	17	6	52	159.42	179	1022.9	13.415	0.0210		0.16	
A	17	6	102	159.92	179.5	1025.7	14.140	0.3530		2.50	
B	1	1	2	0.02	0.02	0.1	6.880	0.0370		0.54	
B	1	1	52	0.52	0.52	3.0	7.266	0.0160	0.0030	0.22	0.04
B	1	2	2	1.52	1.52	8.7	6.302	0.0220		0.35	
B	1	3	2	3.02	3.02	17.3	7.261	0.0230		0.32	
B	1	3	52	3.52	3.52	20.1	7.478	0.0100		0.13	
B	1	3	102	4.02	4.02	23.0	7.198	0.0120		0.17	
B	1	4	52	5.02	5.02	28.7	8.361	0.0050		0.06	
B	1	5	52	6.52	6.52	37.3	9.215	0.1000		1.09	
B	1	6	2	7.52	7.52	43.0	13.392	0.0020	0.0230	0.01	0.17
B	2	2	52	10.32	10.94	62.5	8.584	0.6280	0.0410	7.32	0.48
B	2	3	2	11.32	11.94	68.2	13.332	0.7740	0.2410	5.81	1.81
B	2	3	52	11.82	12.44	71.1	14.726	0.6160	0.5770	4.18	3.92
B	2	3	102	12.32	12.94	73.9	10.091	0.0210		0.21	
B	2	4	2	12.82	13.44	76.8	9.635	0.0150		0.16	
B	2	4	52	13.32	13.94	79.7	9.763	0.0430		0.44	
B	2	4	102	13.82	14.44	82.5	12.569	0.5040		4.01	
B	2	5	52	14.82	15.44	88.2	6.091	0.0450		0.74	
B	2	5	102	15.32	15.94	91.1	10.774	0.1120		1.04	
B	4	5	2	33.32	36.21	206.9	14.636	0.0180		0.12	
B	6	4	102	51.82	57.42	328.1	10.699	0.0310		0.29	
B	7	2	2	57.32	63.87	365.0	10.977	0.3340		3.04	
B	7	4	52	60.76	67.31	384.6	12.535	0.0460		0.37	
B	8	3	102	69.32	76.95	439.7	12.024	0.0270		0.22	
B	9	2	52	76.82	85.53	488.7	14.789	0.0220		0.15	
B	9	2	102	77.32	86.03	491.6	16.261	0.0400		0.25	

B	9	4	52	79.82	88.53	505.9	16.735	0.0240		0.14	
B	9	5	2	80.82	89.53	511.6	17.028	0.0690		0.41	
B	10	4	52	89.32	98.67	563.8	17.174	1.1080	0.0170	6.45	0.10
B	10	5	102	91.32	100.67	575.3	14.337	0.0220		0.15	
B	10	6	2	91.82	101.17	578.1	16.028	0.0050		0.03	
B	10	6	102	92.82	102.17	583.8	16.469	0.0220		0.13	
B	11	3	2	96.81	107.16	612.3	13.482	0.0140		0.10	
B	11	3	52	97.31	107.66	615.2	17.077	0.0240		0.14	
B	11	4	52	98.81	109.16	623.8	16.182	0.0650		0.40	
B	11	4	102	99.31	109.66	626.6	10.964	0.0920		0.84	
B	11	5	2	99.81	110.16	629.5	15.625	0.2350	0.0160	1.50	0.10
B	11	5	52	100.31	110.66	632.3	15.999	0.0680		0.43	
B	11	5	102	100.81	111.16	635.2	15.690	0.5110	0.0380	3.26	0.24
B	11	6	2	101.31	111.66	638.1	12.288	0.1910		1.55	
B	11	6	52	101.81	112.16	640.9	13.884	0.0120		0.09	
B	11	6	102	102.31	112.66	643.8	14.535	0.0020		0.01	
B	12	4	102	108.77	119.63	683.6	19.506	0.0610		0.31	
B	12	5	2	109.26	120.12	686.4	19.758	0.0970		0.49	
B	12	5	102	110.26	121.12	692.1	17.748	0.0520		0.29	
B	17	4	2	155.27	170.67	975.3	15.938	0.0120		0.08	
B	17	4	102	156.27	171.67	981.0	5.811	0.0210		0.36	
B	17	5	2	156.74	172.14	983.7	13.927	0.0220		0.16	
B	17	5	52	157.24	172.64	986.5	14.417	0.0170		0.12	
B	17	5	102	157.74	173.14	989.4	16.691	0.0060		0.04	
B	17	6	2	158.23	173.63	992.2	14.057	0.0580		0.41	
B	18	3	2	163.28	179.58	1026.2	12.173	0.0250		0.21	
B	18	3	52	163.78	180.08	1029.0	14.357	0.0040		0.03	
B	18	3	102	164.28	180.58	1031.9	14.900	0.0050		0.03	
B	18	4	2	164.78	181.08	1034.7	8.586	0.0940	0.0590	1.09	0.69

B	18	4	52	165.28	181.58	1037.6	13.925	0.0250		0.18	
B	18	4	102	165.78	182.08	1040.5	14.997	0.0220		0.15	
B	18	5	2	166.29	182.59	1043.4	14.839	0.0040		0.03	
C	6	6	2	51.22	55.11	314.9	9.590	0.0710		0.74	
C	12	3	52	104.22	113.42	648.1	14.560	0.2430		1.67	
C	12	3	102	104.72	113.92	651.0	14.185	0.0800		0.56	
C	12	4	102	106.22	115.42	659.5	15.443	0.0690		0.45	
C	12	5	52	107.22	116.42	665.3	13.604	0.0660		0.49	
C	12	5	102	107.72	116.92	668.1	13.674	0.0250		0.18	
C	12	6	2	108.22	117.42	671.0	15.141	0.0330		0.22	
C	12	6	52	108.72	117.92	673.8	14.261	0.0310		0.22	
C	12	6	102	109.22	118.42	676.7	12.797	0.0260		0.20	
C	14	2	2	121.22	132.88	759.3	11.914	0.0890	0.2470	0.75	2.07
C	14	2	52	121.72	133.38	762.2	15.230	0.0180		0.12	
C	14	3	2	122.72	134.38	767.9	10.260	0.0840		0.82	
C	14	3	52	123.22	134.88	770.7	11.222	0.0220		0.20	
C	14	3	102	123.72	135.38	773.6	10.500	0.0920		0.88	
C	14	4	2	124.22	135.88	776.5	11.736	0.0160		0.14	
C	14	4	52	124.72	136.38	779.3	12.644	0.4790		3.79	
C	14	5	2	125.72	137.38	785.0	12.342	0.0500		0.41	
C	14	5	52	126.22	137.88	787.9	16.170	0.0040		0.02	
C	14	5	102	126.72	138.38	790.7	14.253	0.0340		0.24	
C	14	6	2	127.22	138.88	793.6	12.354	0.0060		0.05	
C	14	6	52	127.72	139.38	796.5	10.793	0.0720		0.67	
C	14	7	2	128.72	140.38	802.2	13.299	0.6050	0.5210	4.55	3.92

** Sample ages to depth were calculated using a average mean sedimentation rate of 17 cm/k.y. - determined by the 303 Scientific Party